Colloids and Surfaces B: Biointerfaces 114 (2014) 164–169

Contents lists available at ScienceDirect

Colloids and Surfaces B: Biointerfaces

journal homepage: www.elsevier.com/locate/colsurfb

Direct electrochemistry and electrocatalysis of glucose oxidase immobilized on reduced graphene oxide and silver nanoparticles nanocomposite modified electrode

Selvakumar Palanisamy, Chelladurai Karuppiah, Shen-Ming Chen *

Department of Chemical Engineering and Biotechnology, National Taipei University of Technology, No. 1, Section 3, Chung-Hsiao East Road, Taipei 106, Taiwan, ROC

ARTICLE INFO

Article history:
Received 7 June 2013
Received in revised form 2 October 2013
Accepted 4 October 2013
Available online 16 October 2013

Keywords:
Reduced graphene oxide
Silver nanoparticles
Direct electron transfer
Glucose oxidase
Glucose biosensor

ABSTRACT

The direct electrochemistry of glucose oxidase (GOx) was successfully realized on electrochemically reduced graphene oxide and silver nanoparticles (RGO/Ag) nanocomposite modified electrode. The fabricated nanocomposite was characterized by field emission scanning electron microscope and energy dispersive spectroscopy. The GOx immobilized nanocomposite modified electrode showed a pair of well-defined redox peaks with a formal potential (E°) of −0.422 V, indicating that the bioactivity of GOx was retained. The heterogeneous electron transfer rate constant (K_s) of GOx at the nanocomposite was calculated to be 5.27 s^{-1}, revealing a fast direct electron transfer of GOx. The GOx immobilized RGO/Ag nanocomposite electrode exhibited a good electrocatalytic activity toward glucose over a linear concentration range from 0.5 to 12.5 mM with a detection limit of 0.16 mM. Besides, the fabricated biosensor showed an acceptable sensitivity and selectivity for glucose.

1. Introduction

The direct electrochemistry of redox proteins have received considerable interest due to their key role in electrochemical biosensors [1] and biofuel cells [2]. Electrochemical analysis provides a powerful platform to investigate the electrochemical communication between the redox active enzymes and electrode surface [3]. Among various enzymes, glucose oxidase (GOx) is one of the well-known redox active enzyme that has been widely used as a model enzyme for the electrocatalysis of glucose [4]. However, direct electron transfer (DET) of GOx at bare and conventional electrodes are impossible, because the redox active site of GOx is deeply buried inside the enzyme matrix [5]. In order to improve the DET of GOx, nanomaterials modified electrodes have been widely used [6]. On the other hand, reduced graphene oxide (RGO) with its high surface area and good conductivity has become one of the imperative nanomaterial that has been increasingly used in various potential applications, particularly in electrochemical sensors and biosensors [7]. However, the DET of GOx on RGO matrix is still a challenging task to be overcome. Thus, many approaches have been developed to immobilize GOx on the RGO surface to attain the better DET [8]. Recently, various nanoparticles have been decorated directly on the RGO surface to enhance the sensitivity of RGO [9]. Among various nanoparticles, silver nanoparticles (Ag) have good conductivity and biocompatibility. Thus, they have been widely used in the electrocatalysis of biomolecules, medical diagnosis and biomedical therapies [10]. Ag were decorated directly on the RGO surface through electrochemical or chemical routes. Generally, RGO/Ag nanocomposite has been prepared using reducing agents [11]. On the other hand, electrochemical methods have received considerable interest, because they are simple and eco-friendly. When compared with other chemical methods, they are more green and facile and no hazardous chemicals and reagents are required [12]. Thus, they are considered as alternative for the preparation of RGO/Ag nanocomposite. However, reports on the electrochemical preparation of RGO/Ag nanocomposite without using any additional reducing agents are limited [13]. To the best of our knowledge, RGO/Ag nanocomposite has never been used for the immobilization of redox active proteins.

Herein, we investigated the direct electrochemistry of GOx on electrochemically prepared RGO/Ag nanocomposite modified electrode. The GOx immobilized nanocomposite electrode displayed good electrocatalytic activity toward glucose with good sensitivity. The high surface area and good biocompatibility of the RGO/Ag nanocomposite provides good microenvironment for GOx, leading to rapid direct electronic communication between GOx and the electrode surface.

* Corresponding author. Tel.: +886 2270 17147; fax: +886 2270 25238.
E-mail address: smchen78@ms15.hinet.net (S.-M. Chen).

0927-7765/$ – see front matter © 2013 Elsevier B.V. All rights reserved.
http://dx.doi.org/10.1016/j.colsurfb.2013.10.006

2. Experimental

2.1. Materials

Raw graphite was purchased from Sigma–Aldrich. $AgNO_3$ and D(+) glucose were received from Aldrich. Prior to real sample analysis, urine samples were diluted with pH 7 solution. The pH 7 (PBS) solution was prepared using 0.05 M Na_2HPO_4 and NaH_2PO_4 solutions and the final pH was adjusted with 0.5 M H_2SO_4 and 2 M NaOH. All other chemicals used were of analytical grade and solutions were prepared with Millipore water.

2.2. Apparatus

All electrochemical measurements including cyclic voltammetry (CV) were carried out using CHI 750a electrochemical analyzer (CH instruments). Surface morphological studies were carried out using a Hitachi S-3000H scanning electron microscope (SEM) and Hitachi field emission scanning electron microscope (FESEM). Elemental analysis (EDX) was studied using HORIBA EMAX X-ACT energy-dispersive X-ray spectrometer. Electrochemical impedance spectroscopy (EIS) studies were performed using IM6ex ZAHNER (Kronach, Germany). A conventional three-electrode system was employed for electrochemical experiments. GCE with an active surface area of 0.079 cm^2 was used as a working electrode. Ag/AgCl electrode (Sat. KCl) and platinum wire with 0.5 mm diameter were used as reference and counter electrodes, respectively. All electrochemical measurements were carried out at room temperature and electrolytes in the electrochemical cell were kept under a nitrogen (N_2) atmosphere (except electrocatalysis of glucose).

2.3. Fabrication of the biosensor

Graphene oxide (GO) was prepared according to the procedure described in our previous work [14]. To prepare RGO/Ag nanocomposite, about 1 ml of GO solution (0.5 mg ml^{-1}) was mixed with 2 ml of 0.5 mM $AgNO_3$ aqueous solution. The obtained mixture was bath sonicated at room temperature for 10 min to obtain a stable aqueous dispersion. Then, this dispersion was centrifuged at 2000 rpm to remove the loosely bounded silver ions on GO sheets. About 8 μl (optimum concentration) of GO/Ag dispersion was drop casted on a pre-cleaned GCE surface, and dried in an air oven. The GO/Ag dispersion modified GCE was transferred into an electrochemical cell containing pH 5 solution. 20 successive cyclic voltammograms were performed from 0 to −1. 4 V at the scan rate of 50 mV s^{-1}. During the successive cycles, GO/Ag was electrochemically reduced to RGO/Ag nanocomposite. Similarly, RGO modified electrode was electrochemically prepared without $AgNO_3$ dispersion.

Fresh GOx (5 mg ml^{-1}) solutions were prepared in PBS and stored at 4 °C. To immobilize GOx, about 6 μl of GOx was drop casted on a RGO/Ag nanocomposite modified electrode and allowed to dry at room temperature. The enzyme immobilized nanocomposite electrode was stored at 4 °C when not in use.

3. Results and discussion

3.1. Characterization of RGO/Ag nanocomposite

Fig. 1A illustrates the surface morphology of electrochemically prepared RGO/Ag nanocomposite. The FESEM image of RGO/Ag nanocomposite reveals that Ag with an average diameter of 70 ± 5 nm are closely anchored on the RGO sheets. Whereas, ultra thin sheets of RGO are closely attached with each other (inset). The surface morphological studies clearly show that electrochemical reduction is an effective and simple method to deposit Ag more uniformly on RGO sheets. We also studied the effect of $AgNO_3$ concentrations on the growth of Ag particles on GO surface using a constant concentration of GO. Fig. S1 displays SEM images of RGO/Ag nanocomposite prepared using 0.3, 0.5 and 0.8 mM $AgNO_3$. It is evident that more Ag are deposited on the RGO surface when $AgNO_3$ concentration was increased from 0.3 to 0.8 mM. Further increases in $AgNO_3$ concentration may lead to aggregation of nanoparticles. The optimal $AgNO_3$ concentration to be used for the uniform distribution of Ag on the GO surface is 0.5 mM. Fig.S2A and B shows FESEM images of the GOx immobilized RGO/Ag nanocomposite at low and high resolutions, respectively. It can be seen that GOx with the shapes of flakes and spheres are immobilized on the surface of RGO/Ag nanocomposite, confirming that RGO/Ag provides a suitable platform for the immobilization GOx without altering the structure of nanocomposite. The RGO/Ag nanocomposite was further confirmed by the elemental analysis. Fig. 1B and C shows a typical EDX profiles of GO/Ag and RGO/Ag nanocomposite. It is clearly evident that after electrochemical reduction, the oxygen functionalities of GO in RGO/Ag nanocomposite were reduced to 30%. While, a sharp peak of metallic Ag found in the EDX spectrum of RGO/Ag nanocomposite confirmed the presence of Ag in the nanocomposite. On the other hand, GO/Ag composite had higher oxygen content than RGO/Ag nanocomposite, which further reveals the effective reduction of GO/Ag to RGO/Ag nanocomposite. EIS was used to monitor the electrochemical impedance changes at the different film modified GCEs. Fig. 1D shows the EIS of bare (a), RGO (b) and RGO/Ag (c) modified GCEs in PBS containing 5 mM $Fe(CN)6^{3-/4-}$ and 0.1 M KCl. The inset in Fig. 1D shows the Randles equivalent circuit model used for EIS analysis. The total electrode impedance corresponds to the electron transfer resistance (R_{ct}) in series with the parallel connection of the double layer capacitance (C_{dl}) and Wardburg impedance (Z_w). In general, a semicircle portion results from the parallel combination of R_{ct} and C_{dl}. RGO/Ag nanocomposite had a lower R_{ct} value than that of bare and RGO modified electrodes, revealing its faster electron transferring ability. The superior conductivity of RGO and Ag lead to faster electron transfer at the nanocomposite modified electrode surface.

3.2. Formation mechanism of RGO/Ag nanocomposite

The RGO/Ag nanocomposite was prepared through the electrochemical reduction of GO/Ag on GCE. It is well known that GO contains plenty of epoxide and hydroxyl groups on its basal plane, and carbonyl and carboxyl groups on its edge plane. These functional groups act as anchoring sites for Ag^+ in $AgNO_3$ dispersion. Moreover, GO/Ag composite was formed through the Vander Waals interaction between the negatively charged GO and Ag^+ [15]. Fig. 1E shows the cyclic voltammogram of GO/Ag modified electrode recorded from 0 to −1.4 V at the scan rate of 50 mV s^{-1} in pH 5 solution. During the first cycle, a sharp cathodic peak appears at −1.22 V with an onset potential of −0.78 V, which is attributed to the presence of oxygen functionalities on the GO surface [12]. In subsequent cycles, this cathodic peak disappeared completely due to the effective reduction of oxygen functionalities on the GO surface [12]. While, another broad cathodic peak at −0.23 V was noticed in the first cycle. However, this peak disappeared in the subsequent cycles owing to the formation of metallic Ag [13]. When reducing only GO in the same potential window, we did not notice any cathodic peak at −0.23 V, which further confirmed that it belongs to Ag^+ (Fig. 1E inset). The above results clearly confirmed the formation of RGO/Ag nanocomposite.

3.3. Direct electrochemistry of GOx

The direct electrochemistry of GOx immobilized at different modified electrodes was investigated using cyclic voltammetry.

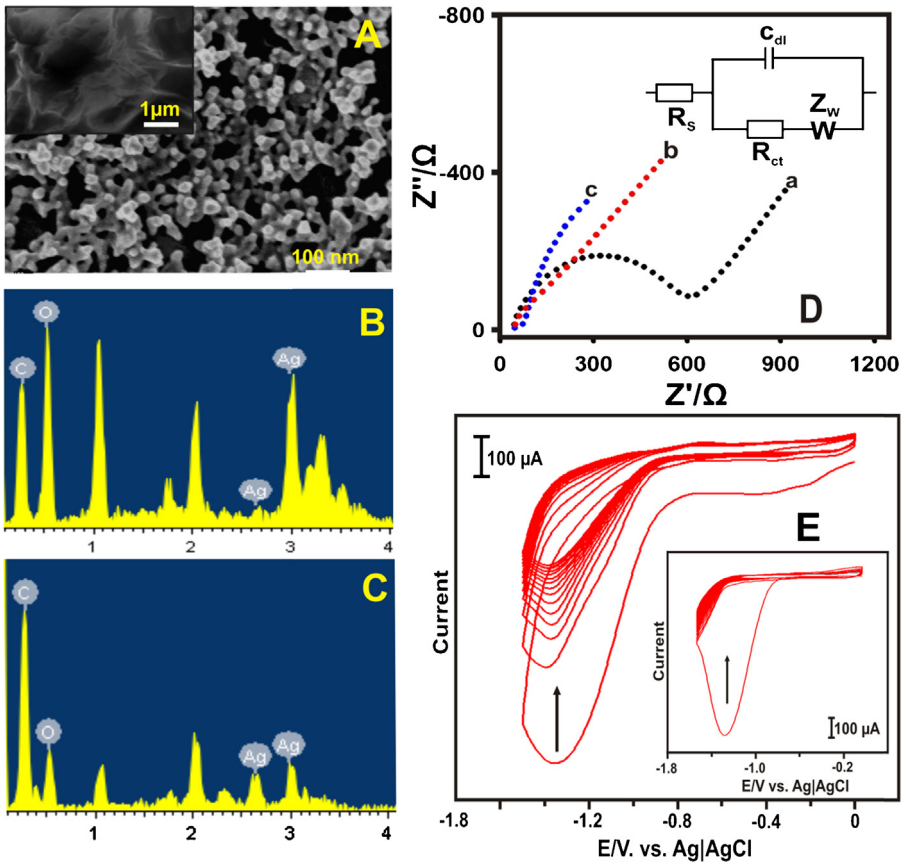

Fig. 1. (A) A typical FESEM image of electrochemically prepared RGO/Ag nanocomposite and SEM image of RGO (inset). The corresponding EDX spectrum of GO/Ag (B) and RGO/Ag (C). (D) EIS of bare (a), RGO (b) and RGO/Ag (c) modified GCEs in PBS containing 5 mM $Fe(CN)6^{3-/4-}$ and 0.1 M KCl. The Randles equivalent circuit model used for EIS analysis (inset). (E) 20 consecutive cyclic voltammograms performed at GO/Ag modified GCE in pH 5 solution at the scan rate of 50 mV s^{-1}. Cyclic voltammograms of GO/GCE recorded under same same conditions (inset).

Fig. 2 shows cyclic voltammograms of GCE/GOx (a), RGO/GOx (b), RGO/Ag (c) and RGO/Ag/GOx (d) modified electrodes in N_2 saturated PBS at the scan rate of 50 mV s^{-1}. The GOx immobilized RGO/Ag modified GCE shows a well-defined redox peak with a formal potential (E_0) of −0.422 V, which is attributed to the reversible

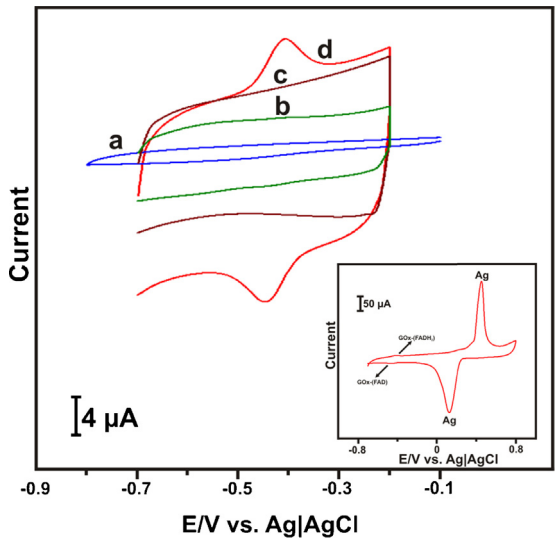

Fig. 2. (A) Cyclic voltammograms of bare GCE/GOx (a), RGO/GOx/GCE (b), RGO/Ag/GCE (c) and RGO/Ag/GOx/GCE (d) in N_2 saturated PBS at the scan rate of 50 mV s^{-1}. Cyclic voltammogram of RGO/Ag/GOx modified GCE obtained in the potential range from 0.8 to −0.7 V in N_2 saturated PBS at 50 mV s^{-1} scan rate (inset).

electron transfer of redox active centers ($FADH_2$, FAD) in GOx [16]. The peak to peak separation (ΔE_p) was found to be 35 mV. The smaller ΔE_p value demonstrates faster direct electron kinetics of GOx at the nanocomposite modified electrode surface. Furthermore, two sharp peaks found at 0.125 and 0.453 V are attributed to the redox behavior of metallic Ag (Fig. 2 inset). In addition, RGO/Ag nanocomposite modified electrode had more capacitance than RGO modified electrode, which further confirms that Ag plays a significant role with RGO in facilitating the electron transfer. However, other modified electrodes did not show any characteristic electrochemical signals for GOx.

3.4. Effect of scan rate and pH

Fig. 3A shows the effect of scan rates on the RGO/Ag/GOx modified electrode. The redox peak current (I_p) and peak potentials (E_p) had a linear dependence with scan rates from 10 to 100 mV (inset), showing that the redox reaction of GOx at the composite electrode is a typical surface-controlled reversible process. Further, the heterogeneous electron transfer rate constant (k_s) of GOx immobilized RGO/Ag composite was calculated to be 5.27 s^{-1} using Laviron's equation (1) [17].

$$\text{Log } k_s = \alpha \text{Log}(1-\alpha) + (1-\alpha)\text{Log}\,\alpha - \text{Log}\left(\frac{RT}{nF\nu}\right) - \alpha(1-\alpha)nF\Delta Ep/2.3RT \quad (1)$$

where R is the gas constant (8.314 J mol^{-1} K^{-1}), T is the room temperature (298.15 K) and ΔE_p is the peak separation of the FAD/$FADH_2$ redox couple. Here, α value is assumed as 0.5 and the

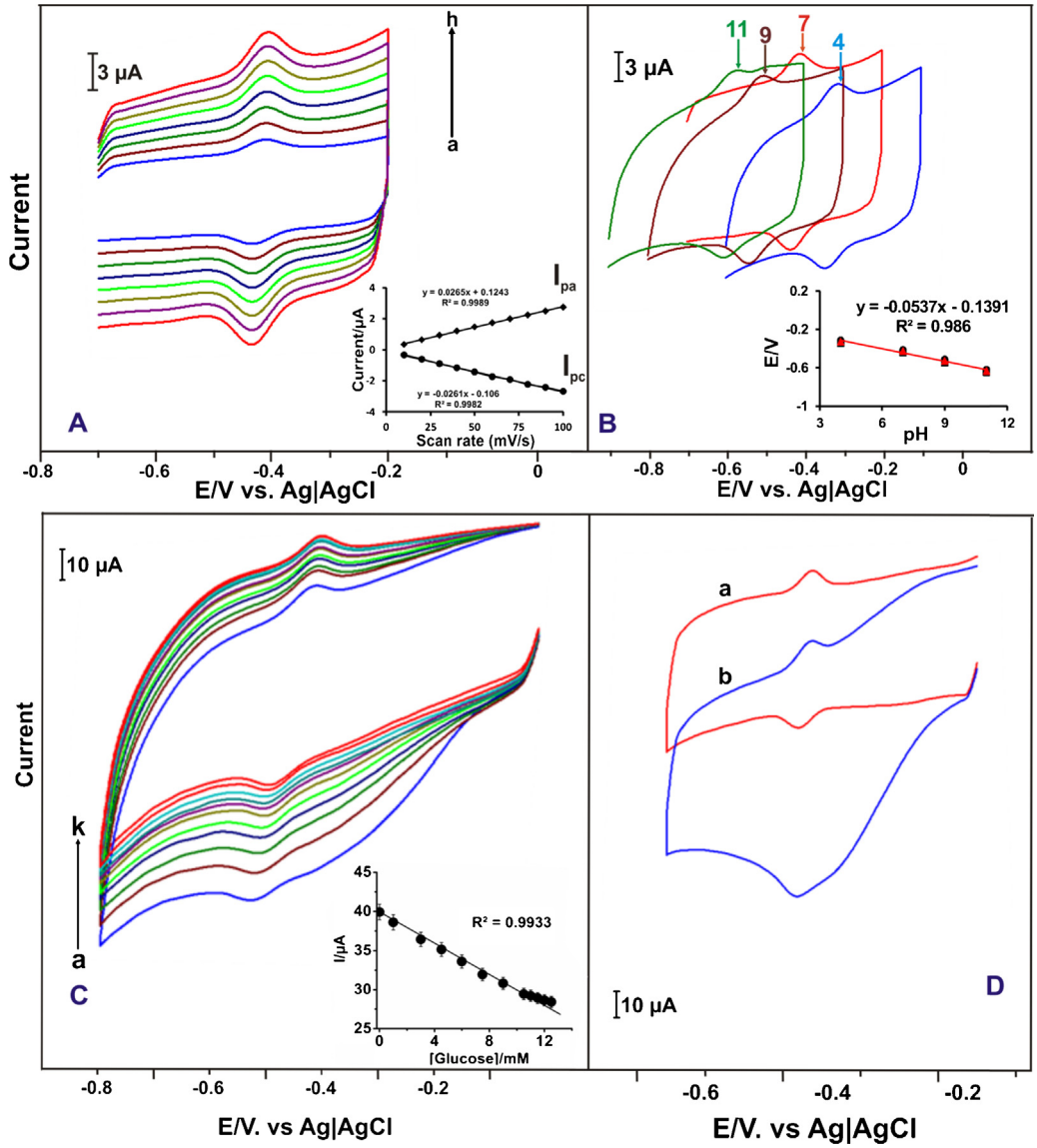

Fig. 3. (A) Cyclic voltammograms of RGO/Ag/GOx modified GCE in N_2 saturated PBS at different scan rates (10–100 mV s^{-1}). Linear dependence of I_p vs. scan rate (inset). (B) CVs of RGO/Ag/GOx modified GCE in various pH (4–11) solutions at 50 mV s^{-1} scan rate. Linear dependence of E_p with pH (inset). (C) Cyclic voltammograms of RGO/Ag/GOx modified GCE in O_2 saturated PBS (pH 7) containing 0.5–12.5 mM glucose (a–k). Error bar represents the relative standard deviation for 3 independent measurements. Inset shows the calibration curve for I_{pc} vs. [glucose]. (D) Cyclic voltammograms obtained at RGO/Ag/GOx modified GCE in N_2 (a) and O_2 (b) saturated PBS at the scan rate of 50 mV s^{-1}.

number of electrons (n) transferred is considered as 2. The K_s value of the GOx immobilized RGO/Ag nanocomposite was higher than that of GOx/RGO (4.8 s^{-1}) [18], graphene/chitosan (2.83 s^{-1}) [19], electrochemically reduced graphene oxide (ERGO)/poly L-lysine (3.27 s^{-1}) [20], multiwalled carbon nanotubes/ERGO (3.02 s^{-1}) [21], graphene/nafion/Au (1.96 s^{-1}) [22] and graphene/nafion (3.42 s^{-1}) [23] modified electrodes. However, the K_s value was lower than that of GOx immobilized on carboxyl terminated poly amido amine dendrimer (PAMAM) modified RGO/Ag composite electrode (8.59 s^{-1}) [24]. The high conductivity and good microenvironment of the RGO/Ag nanocomposite facilitates the direct electron transfer between the enzyme matrix and the electrode surface.

Fig. 3B shows the effect of pH at GOx immobilized RGO/Ag nanocomposite electrode. The peak current at the RGO/Ag nanocomposite electrode in pH 7 solution was found to be higher than that of other pH solutions. Moreover, E_p had a linear dependence with pH values from 4 to 11 (inset). The calculated slope value was found to be in close agreement with the theoretical slope value for a reversible electron transfer process with an equal number of protons and electrons according to Eq. (2) [25]. This result confirmed that the redox reaction of GOx at nanocomposite modified electrode involves an equal number of protons (H^+) and electrons (e^-).

$$\text{GOx-(FAD)} + 2e^- + 2H^+ \leftrightarrow \text{GOx-(FADH}_2\text{)} \quad (2)$$

3.5. Electrocatalysis of glucose

Fig. 3C displays cyclic voltammograms obtained at the RGO/Ag/GOx nanocomposite modified electrode in the presence of different concentrations of glucose in oxygen saturated PBS at the scan rate of 50 mV s^{-1}. A defined reduction peak current (I_{pc}) was observed at −0.492 V in the absence of glucose. Upon increasing the glucose concentration in PBS, I_{pc} decreased, while, the oxidation peak current (I_{pa}) increased, displaying a typical electrocatalysis

Table 1
Comparison of the analytical performance of the proposed GOx immobilized RGO/Ag nanocomposite electrode with other GOx modified electrodes reported previously.

Modified electrode	K_s (s^{-1})	Sensitivity ($\mu A\,mM^{-1}\,cm^{-2}$)	Linear range (mM)	Reference
RGO[a]/GOx[b]	4.8	1.85	0.1–27	[18]
GOx/graphene/CS[c]	2.83 ± 0.18	37.93	0.08–12	[19]
GOx/ERGO[d]/PLL[e]	3.273	NA[f]	0.25–5	[20]
ERGO-MWCNT[g]/GOx/Nf[h]	3.02	7.95	0.01–6.5	[21]
Nf/graphene/GOx/Au[*]	1.96	21.9	2–14	[22]
GOx/graphene/Nf	3.42 ± 0.08	NA	0.5–14	[23]
RGO/PAMAM[i]/Ag[j]/GOx/CS	8.59	75.72	0.032–1.89	[24]
RGO/ZnO[k]/GOx	NA	18.97	0.02–6.24	[26]
GOx/Pd[l]/RGO	NA	14.1	NA	[27]
GOx/graphene	NA	3	0.1–10	[28]
GOx/GO[m]	NA	8.045	Up to 28	[29]
RGO/Ag/GOx	5.27	3.84	0.5–12.5	This work

[a] RGO, reduced graphene oxide.
[b] GOx, glucose oxidase.
[c] CS, chitosan.
[d] ERGO, electrochemically reduced graphene oxide.
[e] PLL, poly L-lysine.
[f] NA, not available.
[g] MWCNT, multiwalled carbon nanotubes.
[h] Nf, nafion.
[i] PAMAM, carboxyl terminated poly amido amine dendrimer.
[j] Ag, silver nanoparticles.
[k] ZnO, zinc oxide.
[l] Pd, palladium nanoparticles.
[m] GO, graphene oxide.
[*] Au, gold electrode.

of glucose at GOx immobilized nanocomposite modified electrode [19]. The mechanism of reduction of dissolved oxygen and oxidation of glucose by GOx is shown in Eq. (3)

$$\text{GOx-(FAD)} + \text{Glucose} + O_2 \rightarrow \text{GOx-(FAD)} + \text{Gluconolactone} + H_2O_2 \quad (3)$$

The I_{pc} decreased linearly when increasing glucose concentrations from 0.5 to 12.5 mM. The correlation coefficient is 0.997 (inset). Upon glucose oxidation, the oxidation peak potential was shifted toward the positive direction, which is attributed to the direct electron transfer of GOx being effectively participating in the glucose oxidation. The limit of detection (S/N = 3) was found to be 0.16 mM. The sensitivity is 3.84 $\mu A m M^{-1} cm^{-2}$. The comparison of the analytical performance of the proposed biosensor with that of previously reported GOx immobilized graphene based electrodes is provided in Table 1. It is evident from Table 1 that the performance of our proposed sensor is comparable with that of other GOx immobilized graphene composite modified electrodes [18–23,26–29]. Under the same experimental conditions, the activity of the GOx immobilized nanocomposite modified electrode was examined in N_2 and O_2 saturated PBS in the absence of glucose. As shown in Fig. 3D, maximum I_{pc} was observed in the presence of O_2 (curve a). While, I_{pc} decreased drastically in the presence of N_2 (curve b). Moreover, the direct electron transfer of GOx dramatically increased in the presence of O_2. GOx catalyzed O_2 and glucose according to Eqs. (4), (5), and (6), respectively.

$$\text{GOx-(FAD)} + 2e^- + 2H^+ \leftrightarrow \text{GOx-(FADH}_2\text{)} \quad (4)$$

$$\text{GOx-(FADH}_2\text{)} + O_2 \rightarrow \text{GOx-(FAD)} + H_2O_2 \quad (5)$$

$$\text{GOx-(FADH}_2\text{)} + \text{Glucose} + O_2 \rightarrow \text{GOx-(FAD)} + \text{Gluconolactone} + H_2O_2 \quad (6)$$

This result clearly validates that RGO/Ag nanocomposite provides a good microenvironment for the fast direct electron transfer of GOx. The high bioreactivity of GOx at the nanocomposite electrode facilitates the electrocatalysis of glucose.

3.6. Selectivity and practicality of the biosensor

The selectivity of the biosensor was investigated using amperometry. The electrode potential was held at −0.49 V (from the CV studies of glucose oxidation) and O_2 saturated PBS was constantly stirred during the experiments. To demonstrate the selectivity of the proposed biosensor, potential interfering biologically active species like dopamine (DA), ascorbic acid (AA) and uric acid (UA) were chosen for the selectivity study. The current–time measurements were carried out at the RGO/Ag nanocomposite in the presence of 2 mM glucose. 1 mM DA, AA and UA were sequentially injected into the same solution at different time intervals. The addition of DA lead to 0.6% current increment, whereas AA and UA did not show any current increments. This result indicates that the proposed biosensor is suitable for practical applications. Moreover, it can be used for the real time sensing of glucose in the presence of excess amounts of interfering species. To evaluate the practicality the fabricated biosensor, enzyme immobilized nanocomposite modified electrode was used for the determination of glucose present in urine samples. The real sample analysis was carried out using the standard addition method [18] and the recovery results are summarized in Table 2. The good recovery results (~97%) validate that the fabricated biosensor electrode can be used for practical applications.

In order to evaluate the storage stability of biosensor, it was stored in 4 °C and its cathodic current was monitored

Table 2
Determination of glucose in human urine samples using the RGO/Ag nanocomposite modified electrode.

Sample	Added (mM)	Found[a] (mM)	Recovery (%)	RSD[b] (%)
A	2	1.92	96	3.9
B	4	3.89	97.2	3.5
C	6	5.96	99.3	4.4

A, B, C, samples of glucose in urine.
[a] Standard addition method.
[b] Relative standard deviation for 3 replicate measurements.

periodically. The biosensor retained about 87.3% of its initial current response even after two weeks, revealing good stability of the biosensor. In order to examine the regeneration ability of the biosensor, we performed seven repeated glucose (2 mM) measurements under the optimized experimental conditions. The RSD for seven repeated glucose measurements is calculated to be 6.2%. The RSD for the determination of 2 mM glucose at five nanocomposite modified electrodes is 4.4%, which validates its good reproducibility. The results clearly indicate that the proposed biosensor has good repeatability and reproducibility.

4. Conclusions

In conclusion, we successfully immobilized GOx on an electrochemically prepared RGO/Ag nanocomposite modified electrode. GOx showed an enhanced direct electrochemistry on the nanocomposite electrode surface. The Ag decoration was of uniform size on the RGO, indicating that electrochemical reduction is an efficient method for the preparation of RGO/Ag nanocomposite. The RGO/Ag nanocomposite provided a good microenvironment for the immobilization of GOx, thus facilitating the electrocatalysis of glucose. The fabricated biosensor showed a good linear response toward glucose with good sensitivity. The good recovery results revealed that this biosensor could be used as a potential candidate for real-time monitoring of glucose in urine samples. In addition, RGO/Ag nanocomposite can be used an immobilization matrix for other redox active enzymes.

Acknowledgments

This project was supported by the National Science Council and the Ministry of Education of Taiwan (Republic of China).

Appendix A. Supplementary data

Supplementary data associated with this article can be found, in the online version, at http://dx.doi.org/10.1016/j.colsurfb.2013.10.006.

References

[1] J.J. Gooding, R. Wibowo, J.Q. Liu, et al., J. Am. Chem. Soc. 125 (2003) 9006.
[2] D. Ivnitski, B. Branch, P. Atanassov, et al., Electrochem. Commun. 8 (2006) 1204.
[3] L. Bai, R. Yuan, Y. Chai, et al., Chem. Commun. 48 (2012) 10972.
[4] R. Wilson, A.P.F. Turner, Biosens. Bioelectron. 7 (1992) 165.
[5] S. Liu, H. Ju, Biosens. Bioelectron. 19 (2003) 177.
[6] Z. Zhu, L.G. Gancedo, A.J. Flewitt, et al., Sensors 12 (2012) 5996.
[7] Y. Shao, J. Wang, H. Wu, et al., Electroanalysis 22 (2010) 1027.
[8] Y. Jiang, Q. Zhang, F. Li, et al., Sens. Actuators B 161 (2012) 728.
[9] S. Zhang, Y. Shao, H. Liao, et al., Chem. Mater. 23 (2011) 1079.
[10] C.M. Welch, C.E. Banks, A.O. Simm, et al., Anal. Bioanal. Chem. 382 (2005) 12.
[11] J. Tian, S. Liu, Y. Zhang, et al., Inorg. Chem. 51 (2012) 4742.
[12] H.L. Guo, X.F. Wang, Q.Y. Qian, et al., ACS Nano 3 (2009) 2653.
[13] B. Zhao, Z. Liu, W. Fu, et al., Electrochem. Commun. 27 (2013) 1.
[14] S. Palanisamy, S.M. Chen, R. Sarawathi, Sens. Actuators B 166 (2012) 372.
[15] Y. He, H. Cui, J. Mater. Chem. 22 (2012) 9086–9091.
[16] C. Shan, H. Yang, J. Song, et al., Anal. Chem. 81 (2009) 2378.
[17] E. Laviron, J. Electroanal. Chem. 101 (1979) 19.
[18] B. Unnikrishnan, S. Palanisamy, S.M. Chen, Biosens. Bioelectron. 39 (2013) 70.
[19] X. Kang, J. Wang, H. Wu, et al., Biosens. Bioelectron. 25 (2009) 901.
[20] L. Hua, X. Wu, R. Wang, Analyst 137 (2012) 5716.
[21] V. Mani, B. Devadas, S.M. Chen, Biosens. Bioelectron. 41 (2013) 309.
[22] J. Hui, J. Cui, G. Xu, et al., Mater. Lett. 108 (2013) 88–91.
[23] Y. Zhang, Y. Fan, S. Wang, et al., Chin. J. Chem. 30 (2012) 1163–1167.
[24] Z. Luo, L. Yuwen, Y. Han, et al., Biosens. Bioelectron. 36 (2012) 179.
[25] Q. Liu, X. Lu, J. Li, et al., Biosens. Bioelectron. 22 (2007) 3203.
[26] S. Palanisamy, A.T. Ezhil Vilian, S.M. Chen, Int. J. Electrochem. Sci. 7 (2012) 2153.
[27] N. Cheng, H. Wang, X. Li, et al., Am. J. Anal. Chem. 3 (2012) 312.
[28] P. Wu, Q. Shao, Y. Hu, et al., Electrochim. Acta 55 (2010) 8606.
[29] Y. Liu, D. Yu, C. Zeng, et al., Langmuir 26 (2010) 6158.